A model-free method for extracting interaction potential between protein molecules using small-angle X-ray scattering

Tomonari Sumi[1*], *Hiroshi Imamura*[2], *Takeshi Morita*[2], *and Keiko Nishikawa*[2]

1 Department of Chemistry, Faculty of Science, Okayama University, 3-1-1 Tsushima-Naka, Kita-ku, Okayama 700-8530, Japan.

2 Graduate School of Advanced integration Science, Chiba University, 1-33 Yayoi, Inage, Chiba 263-8522, Japan.

CORRESPONDING AUTHOR

Tomonari Sumi

Phone: +81(Japan)-86-251-7837

e-mail: sumi@okayama-u.ac.jp

ABSTRACT. A small-angle X-ray scattering has been used to probe protein-protein interaction in solution. Conventional methods need to input modeled potentials with variable/invariable parameters to reproduce the experimental structure factor. In the present study, a model-free method for extracting the excess part of effective interaction potential between protein molecules in solutions over an introduced hard-sphere potential by using experimental data of small-angle X-ray scattering is presented on the

basis of liquid-state integral equation theory. The reliability of the model-free method is tested by the application to experimentally derived structure factors for dense lysozyme solutions with different solution conditions [Javid *et al*., Phys. Rev. Lett. **99**, 028101 (2007), Schroer *et al*., Phys. Rev. Lett. **106**, 178102 (2011)]. The structure factors calculated from the model-free method agree well with the experimental ones. The model-free method provides the following picture of the lysozyme solution: there are the stabilization of contact-pair configurations, large activation barrier against their formations, and screened Coulomb repulsion between the charged proteins. In addition, the model-free method will be useful to verify whether or not a model for colloidal system is acceptable to describing protein-protein interaction.

1. Introduction

The small-angle scattering of X-rays and neutrons from proteins in solution can provide useful information about the structure of the single protein and the effective interaction potential as well as spatial correlations between protein molecules [1,2]. The former is encoded in the form factor $P(q)$ and the latters in the structure factor $S(q)$. These functions are of great interest to the structural biology; the form factor $P(q)$ is used to develop three-dimensional structural model of proteins [1,2], whereas the structure factor $S(q)$ inform efforts to crystallize proteins by providing insight into their spatial configuration in solutions [3–17]. The interpretation of small-angle scattering data from solutions of the well studied protein lysozyme had been controversial: whether or not equilibrium clusters of protein molecules are formed in condensed protein solutions [8,13].

The spatial distribution and intermolecular interaction of proteins in solutions provide important information for understanding and predicting protein functions in vivo as well as all practical processes involving proteins. There are various schemes which make use of different models for the intermolecular interaction potentials $V(r)$ and of different liquid-state theories to calculate the structure

factor $S(q)$ [5,7,11-15,17,18]. The Derjaguin–Landau–Verwey–Overbeek (DLVO) theory successfully describes the microstructure and equilibrium phase behavior of charged colloid systems over a wide phase space. Protein-protein interaction potential $V(r)$ can also be modeled by a simple DLVO-type potential as a sum of the contribution from the hard-sphere repulsion $v_{HS}(r)$, the screened Coulomb potential $v_C(r)$, and a Yukawa-type attractive potential $v_A(r)$ that is originated from van der Waals dispersion forces. However, in comparison with colloidal particles, since the size of proteins is nanometer length scale, effects of hydrogen bonding, hydrophobic hydration, and specific ion binding become important on protein-protein interactions. Therefore, the short-range attractive interaction given by the Yukawa-type function $v_A(r)$ should be modified by those effects in protein solutions. In practice, the repulsive potential is uniquely determined by employing the screened Coulomb potential $v_C(r)$, given by given by Verwey and Overbeek [19]

$$v_C(r) = \frac{Z^2 e^2}{4\pi\varepsilon_0\varepsilon_r(1+0.5\kappa d_{HS})^2}\frac{\exp[-\kappa(r-d_{HS})]}{r}, \quad (1)$$

where Z is the net charge on the protein, e the elementary charge, ε_0 the dielectric permittivity of the vacuum, ε_r the dielectric constant of the medium, and d_{HS} is protein's diameter. κ is the reciprocal Debye-Hückel screening length (= $\left[\left(2e^2/\varepsilon_0\right)I/\left(\varepsilon_r k_B T\right)\right]^{1/2}$), where I is the ionic strength, k_B is the Boltzmann constant, and T is the thermodynamic temperature in kelvins. On the other hand, the parameters J_A and d_A that are contained in the following Yukawa-type attractive potential $v_A(r)$ can be used to fit the calculated $S(q)$ to the experimental small-angle scattering data, [20]

$$v_A(r) = -J_A\left(d_{HS}/r\right)e^{-(r-d_{HS})/d_A}. \quad (2)$$

In general the assumption of a specific model potential can work well in some cases [7] but it might provide an artificial interaction potential if the model potential would not have enough the degree of freedom in the potential form. For instance, the DLVO model could provide good description of $V(r)$ if the contribution of $v_C(r)$ to $V(r)$ is dominant, but the DLVO model would not be sufficient if the Yukawa-

type function $v_A(r)$ can not reproduce the other contributions to $V(r)$ except for $v_C(r)$.

In the study presented here, a model-free method for investigating protein interactions as well as radial distribution function of proteins in solutions are presented. This method is based on a liquid-state integral equation theory using experimental $S(q)$ as the input instead of the introduction of a specific potential model. In order to check the reliability of the model-free method, we applied this method to experimental $S(q)$ data of dense lysozyme solutions that were taken from the literatures [12,15]. Interestingly, the literature [15] reported that pressure dependence of the protein-protein interaction potential is nonlinear. We also analyzed the experimental $S(q)$ by our method, and discussed the physicochemical pictures.

2. Theory

In this section, we present an integral equation approach to solve an inverse problem of the effective interaction potential between protein molecules $V(r)$ in solutions by using experimental structure factor $S_{exp}(q)$ as the input. The excess part of $V(r)$ over hard-sphere interaction potential $v_{HS}(r)$ that is introduced as a reference system is defined by

$$v_{ex}(r) \equiv V(r) - v_{HS}(r). \tag{3}$$

The radial distribution function of proteins $g(r)$ or the pair correlation function between protein molecules $h(r)= g(r)-1$ is related to the direct correlation function $c(r)$ via the Fourier transform of the Ornstein-Zernike (OZ) equation as follows:

$$\hat{h}(q) = \hat{c}(q) + n_0 \hat{c}(q)\hat{h}(q), \tag{4}$$

where n_0 is the number density of protein, $\hat{h}(q)$ and $\hat{c}(q)$ are the Fourier transform of $h(r)$ and $c(r)$, respectively. We define the excess part of the direct correlation function, $c_{ex}(r)$, as follows:

$$c_{ex}(r) \equiv c(r) - c_{HS}(r), \tag{5}$$

where $c_{HS}(r)$ is a direct correlation function for the reference hard-sphere system interacting via $v_{HS}(r)$ at

the same number density n_0. Here we introduce the following assumption for the excess part of the effective interaction potential between protein molecules:

$$-v_{\mathrm{ex}}(r)/k_{\mathrm{B}}T = c_{\mathrm{ex}}(r), \tag{6}$$

where k_B is the Boltzmann constant and T is temperature. This relation is formally same as the relation introduced in the random phase approximation (RPA). The assumption is asymptotically correct for the long-range behavior of $v_{ex}(r)$. The reliability of applying the assumption for all distances including short distances such as contact-pair distances between protein molecules should be determined by whether or not the model-free method with Eq. (6) can reproduce experimental structure factors. In addition to the RPA-type relation, the following closure relation is also introduced:

$$h(r) = \exp\left[-V(r)/k_{\mathrm{B}}T + \gamma(r) + B(r)\right] - 1, \tag{7}$$

where $\gamma(r) = h(r) - c(r)$ and $B(r)$ is a bridge function that is regarded as a correction for the hyper-netted chain (HNC) approximation where $B(r)$ is zero. In this study, the following Verlet-modified bridge function is employed as $B(r)$ [21, 22]:

$$B(r) = \frac{\gamma^2(r)}{2\left[1 + (4/5)\gamma(r)\right]}, \tag{8}$$

It is well known that the HNC approximation systematically overestimates the value of $S(q)$ at small q-values [23]. In general, the bridge function mainly provides a correction on the overestimate of $S(q)$ at small q-values for the HNC approximation but does not affect short-range structures very much.

Finally, substitution of equations (3), (5), and (6) into Eq. (7) and the use of Eq. (4) gives the following closure relation that we can use to solve the inverse problem of $V(r)$ using experimental structure factor as the input:

$$h(r) = \begin{cases} \exp\left[\gamma_{\mathrm{s}}(r) + B(r)\right] - 1 & r > d_{\mathrm{HS}} \\ -1 & r \le d_{\mathrm{HS}} \end{cases}, \tag{9}$$

where d_{HS} is the diameter of hard-sphere fluid with $v_{\mathrm{HS}}(r)$, e.g. protein's diameter here, and

$\gamma_s(r) = h(r) - c_{HS}(r)$ is provided by the inverse Fourier transform of

$$\hat{\gamma}_s(q) = \hat{c}(q)/\left[1 - n_0\hat{c}(q)\right] - \hat{c}_{HS}(q) \tag{10}$$

with

$$\hat{c}(q) = \hat{h}'(q) - \left[\hat{\gamma}_s(q) - \hat{c}_{ex}(q)\right], \tag{11}$$

where $\hat{h}'(q)$ for $q \le q_h$ is obtained from the experimental data of $S_{exp}(q)$ via $\hat{h}_{exp}(q) = \left[S_{exp}(q) - 1\right]/n_0$, while $\hat{h}'(q)$ for $q > q_h$ is obtained from the Fourier transform of $h(r)$ provided by Eq. (9). The partial displacement in $\hat{h}'(q)$ for $q \le q_h$ with the experimental $\hat{h}_{exp}(q)$ means that the experimental $S_{exp}(q)$ is used as the input of the integral equation instead of information about unknown interaction potential between protein molecules. The value of q_h should be chosen so that the calculated $h(q)$ for $q > q_h$ from the closure relation of Eq. (9) smoothly continues to the experimental $h_{exp}(q)$ at q_h within the experimentally available q-values. Since $v_{ex}(r)$ does not explicitly appear in Eq. (9), we can obtain $v_{ex}(r)$ without any model potential from a self-consistent $c_{ex}(r)$ via Eq. (6) by iteratively solving the integral equation until the Fourier transform of $h(r)$ calculated from Eq. (9) is well converged. The detail of the calculation procedure is shown in the appendix. The hard sphere diameter d_{HS} in $v_{HS}(r)$ was chosen as a minimum contact distance between protein molecules. It is noted that $S(q)$ shown as the theoretical results in figures are the one obtained from the Fourier transform of $h(r)$ that is calculated from the closure relation of Eq. (9) without the partial displacement with $\hat{h}_{exp}(q)$.

3. Computational details

In order to investigate the reliability of the model-free method with the integral equation, we applied the method to lysozyme 10 wt% solutions at 25 ºC and 1bar in 20mM citrate buffer at pH 4.6 [12] and

in 25mM bis-Tris buffer at pH 7 [15]. The maximum q-value for which the experimental $S_{exp}(q)$ values are available is q_h=1.8 nm^{-1} for the citrate buffer solution and q_h=4.0 nm^{-1} for the bis-Tris buffer solution, respectively. The data of $S(q)$s shown in Fig. 1(b) of Ref. 15 is probably a theoretical fitting to experimental $S_{exp}(q)$. However, we do not care about it because the main purpose of the use of these data is for applying the model-free method. In the manuscript, we refer the structure factors that are shown in Fig. 2(b) of Ref. 12 and in Fig. 1(b) of Ref. 15 as the experimental data I and II, respectively. In the experimental data I, since there was no small-angle values of $S_{exp}(q)$ at q-values less than 0.2 nm^{-1}, we prepared the small-angle values of $S_{exp}(q)$ using an extrapolation with a Lorenz-type function in the present analyses. In this study, the integral equation was solved with 4096 grid points, in which the maximum value of the radial distance was 100 nm. In all the theoretical calculations, 2.7 nm is employed as d_{HS} in $v_{HS}(r)$ according to the length of the shorter axis when lysozyme is regarded as an ellipsoid. The number density of protein n_0 is 4.2×10^{-6} Å^{-3} when the protein concentration is 10 wt % (= 0.10 g/mL = 7.0 mM).

3. Results

Figure 1 shows comparison between the reported experimental data [12, 15] and the present theoretical results for $S(q)$ in 10 wt % lysozyme solution. The theoretical results agree well with the experimental $S_{exp}(q)$ data I and II, respectively. Especially, both the low-q and high-q peaks in $S(q)$ for Exp. data II can be reproduced by the model-free method. In comparison with Exp. data II, the model-free method provides the smaller peak at the high-q region for Exp. data I. It is noted that the theoretical $S(q)$ that is calculated from the Fourier transform of $h(r)$ given by Eq. (9) is deviated from the experimental $S_{exp}(q)$ even though $S_{exp}(q)$ is used as the input. The deviation should be attributed to the assumption of Eq. (6).

Figures 2(a) and 2(b) show theoretical results of the radial distribution functions of proteins $g(r)$ and the effective interaction potentials between protein molecules $V(r)$, respectively. A significant first peak

that indicates the contact-pair configurations is observed in $g(r)$ for Exp. data II, while a smaller first peak in $g(r)$ whose height is less than 1 is provided for Exp. data I. These observations strongly suggest that the experimental data at the high-q region affects the microscopic structures in the small length scale comparable with the size of protein. Except for the first maximum, the asymptotic behavior of $g(r)$ for those Exp. data at the distances larger than the first maximum qualitatively agrees each other: both $g(r)$s increase from values less than 1 with the increase in the distance.

In Fig. 2(b), we can see again that the relative stabilization of the contact-pair configurations for Exp. data II at the distances around 3.4 nm, whose value is slightly larger than d_{HS}=2.7 nm. A large first peak in $V(r)$ comparable with the same order of k_BT is also found for Exp. data II. The activation barrier against the formation of the contact-pair configurations plays the crucial role on the stability of metastable states of dense protein solutions.

In Fig. 3, pressure dependence of experimental $S_{exp}(q)$ for lysozyme 10 wt% solution at 25 ˚C in bis-Tris buffer [15] is shown. The calculated $S(q)$s from the model-free method are shown in the inset. The values of $S(q)$ for q between 1 and 2 nm^{-1} once increase with the increase in pressure from 1 bar to 1.5 kbar, and then decrease with the further increase in pressure from 1.5 kbar to 3.5 kbar. On the other hand, the values of $S(q)$ for q less than 1 nm^{-1} first decrease with the increase in pressure and then increase with the further increase in pressure from 1.5 kbar to 3.5 kbar. We can see in the inset that the similar pressure dependence of $S(q)$ is reproduced by the model-free method.

Figures 4(a) and 4(b) show pressure dependence of the radial distribution functions of proteins $g(r)$ and the effective interaction potentials between protein molecules $V(r)/k_BT$, respectively. In both $g(r)$ and $V(r)/k_BT$, the long-range behaviors at the distances larger than 4 nm are not significantly affected by the increase in pressure at least less than 3.5kbar. The result could be interpreted by a small pressure effect on the long-range Coulomb repulsion between charged protein molecules. On the other hand the increase in pressure strongly effects the stabilization of the contact-pair configurations of proteins. The contact-pair configurations are destabilized by an increase in pressure from 1 bar to 1.5 kbar and then

gradually stabilized by the farther increase in pressure from 1.5 kbar to 3.5 kbar. In contrast to the smaller pressure effects on the long-range Coulomb interactions, the pressure dependence of the contact-pair stabilization can be attributed to pressure dependence of hydrophobic interactions. The increase in $V(r)/k_BT$ at the contact-pair distances with the increase in pressure up to 1.5 kbar is qualitatively agreed with the result that has been reported by Ortore *et al*. [14].

In Fig. 5, the minimum energy value of $V(r)/k_BT$ at the first minimum and the distance at the first minimum of $V(r)/k_BT$ are respectively shown on the left and right axis as the function of pressure. The first minimum energy value of $V(r)/k_BT$ increases from negative to positive with the increase in pressure from 1 bar to 1.5 kbar and then decreases from positive to negative again with the farther increase in pressure. At the same time, the first minimum distance in $V(r)/k_BT$ first increases and then decreases as pressure increases. The non-linear pressure dependence of the energy value at the first minimum of $V(r)/k_BT$ qualitatively agrees well with results obtained from theoretical analysis with the DLVO model potential for the same experimental $S_{exp}(q)$s.

4. Discussion

As seen in Fig. 1, the high-q data of $S_{exp}(q)$ is available in Exp. data II, while the data of $S_{exp}(q)$ at q-values larger than 1.8 nm^{-1} is absence in Exp. data I. As the result, the model-free method reproduces a larger peak in $S(q)$ at q-values around 2.3 nm^{-1} for Exp. data II but dose not provide a significant peak at this q-region for Exp. data I. At the same time, as seen in Fig. 2(a), the model-free method provides a large first maximum in $g(r)$ for Exp. data II but dose not provide a significant first peak for Exp. data I. The large first maximum in $g(r)$ for Exp. data II indicates the stabilization of contact-pair conformations of proteins. The comparison between theoretical results obtained from these different experimental $S_{exp}(q)$ data clearly shows that the intermolecular microscopic structural information in the length scale comparable with the size of proteins is attributed to the high-q data of $S_{exp}(q)$.

It has been controversial whether or not equilibrium clusters of proteins are formed in dense lysozyme

solutions [8,13]. The effective interaction potential between protein molecules $V(r)$ obtained for Exp. data II from the model-free method shows a large first minimum at the contact distances and a screened Coulomb repulsion [See Fig. 2(b)]. As seen in $g(r)$ obtained for Exp. data II, the large first maximum indicating the stabilization of the contact-pair conformations and the gradual increase in $g(r)$ from values less than 1 with an increase in the radial distance are observed in Fig. 2(a). The shape of $g(r)$ looks like monomer-monomer $g(r)$ in polymer melts. These observations suggest the formation of worm-like clusters consisting of proteins in dense lysozyme solutions.

As seen in $V(r)$ for Exp. data II in Fig. 2(b), the model-free method provides a large first positive maximum in $V(r)$ that disturbs the formation of the contact-pair conformations. The activation energy barrier comparable with k_BT against the contact-pair formation plays a crucial role on the stabilization of protein solutions. In our previous study using a liquid-state-density-functional theory, both the similar stabilization of the contact-pair configurations and the large activation barrier against their formation have been demonstrated by the potential of mean force between hydrophobic/solvophobic large solutes in water/Lennard-Jones (LJ) solvent [24]. If no van der Waals attractive interaction between solute and solvent was taken into account, the activation barrier against the formation of the contact-pair configurations completely disappeared, while the contact-pair configurations were more stabilized. These results suggest that the large activation barrier would be caused by the formation of hydration/solvation shell around large hydrophobic/solvophobic solutes. The model-free method can extract hydration effects on protein-protein interactions from the experimental $S_{exp}(q)$ data.

The model-free method also reproduces the non-linear pressure dependence of the structure factor. The stability of the contact-pair configurations is strongly affected by an increase in pressure, while the screened Coulomb repulsion is not significantly affected by the increase in pressure. The non-linear change in the relative stability of the contact-pair configurations can be attributed to pressure effects on hydrophobic hydration.

5. Conclusion

In the present study, a model-free method for extracting the effective protein-protein interaction potential as well as the radial distribution function of proteins was proposed. This is the theoretical method based on a liquid-state integral equation where experimental structure factor $S_{exp}(q)$ is used as the input instead of introducing a specific model interaction potential between protein molecules such as the DLVO potential. By using this method, we can solve an inverse problem of the effective interaction potential between protein molecules starting from experimental structure factor $S_{exp}(q)$ without any assumption of the specific model potential except for the hard-sphere diameter of introduced reference hard-sphere system. We applied the model-free method to different experimental data of $S_{exp}(q)$ for dense lysozyme solutions. The model-free method can reproduce the experimental $S_{exp}(q)$ very well and provides an useful information about spatial correlations and effective interaction potential between protein molecules in the length scale comparable with the size of protein if the effective experimental data of $S_{exp}(q)$ is available up to enough high-q region. The model-free method shows the stabilization of contact-pair configurations, large activation barrier against their formations, and screened Coulomb repulsion between charged protein molecules. The result suggests the formation of worm-like clusters consisting of proteins.

ACKNOWLEDGMENT. This work was supported in part by Grant-in-Aid for Scientific Research (KAKENHI) (No.25610121) from the Ministry of Education, Culture, Sports, Science and Technology of Japan. H.I. and T.S. also thank Prof. Ryo Akiyama in Kyushu University for useful discussion.

Appendix

The values of $\hat{h}'(q)$ for $q \le q_h$ in Eq. (11) is fixed to be $\hat{h}_{\exp}(q) = \left[S_{\exp}(q) - 1\right]/n_0$ during the iterative calculation for solving the integral equation, while the values of $\hat{h}'(q)$ for $q > q_h$ in Eq. (11) are updated using the Fourier transform of $h(r)$ calculated from Eq. (2). The detailed procedure of the calculation is given as follows:

An initial guess is provided by

$$\hat{h}'(q) = \begin{cases} \hat{h}_{\exp}(q) & q \le q_h \\ \hat{h}_{HS}(q) & q > q_h \end{cases}, \tag{A1}$$

where $\hat{h}_{HS}(q)$ is the one obtained from the hard-sphere reference system, and

$$\hat{\gamma}_s^{old}(q) = \hat{\gamma}_s^{new}(q) = 0, \tag{A2}$$

$$\hat{c}(q) = \hat{c}_{HS}(q), \tag{A3}$$

and

$$\hat{h}_{old}(q) = \hat{h}_{HS}(q). \tag{A4}$$

The following iterative calculation will be continued until the absolute difference between $\hat{h}_{new}(q)$ and $\hat{h}_{old}(q)$ becomes less than a threshold.

1. $\hat{c}_{ex}(q) = \hat{c}(q) - \hat{c}_{HS}(q)$. (A5)

2. $\hat{c}(q) = \hat{h}'(q) - \left[\hat{\gamma}_s(q) - \hat{c}_{ex}(q)\right]$. (A6)

3. $\hat{\gamma}_s(q) = \hat{c}(q)/\left[1 - n_0 c(q)\right] - \hat{c}_{HS}(q)$. (A7)

4. $\hat{\gamma}_s(q) = a\hat{\gamma}_s(q) + (1-a)\hat{\gamma}_s^{old}(q)$, where a is the dumping parameter. (A8)

5. $\hat{\gamma}_s^{old}(q) = \hat{\gamma}_s(q)$. (A9)

6. $h(r) = \begin{cases} \exp\left[\gamma_s(r) + B(r)\right] - 1 & r > d_{HS} \\ -1 & r \le d_{HS} \end{cases}$. (A10)

7. If a difference between $\hat{h}(q)$ and $\hat{h}^{old}(q)$ less than the threshold, go to step 8 (outside the iteration loop), otherwise $\hat{h}_{old}(q) = \hat{h}(q)$ and $\hat{h}'(q) = \hat{h}(q)$ for $q > q_h$, then go back to step 1.

8. $S(q)$ is calculated via $S(q) = 1 + n_0 \hat{h}(q)$.

Figure 1. Comparison between experimental and calculated structure factors $S(q)$ for lysozyme 10 wt % solutions at 25 ºC and 1 bar in 20mM citrate buffer at pH 4.6 and in 25 mM bis-Tris buffer at pH 7. The experimental $S_{exp}(q)$ in the citrate buffer solution is obtained from Fig. 2(b) in Ref. [12]. The experimental $S_{exp}(q)$ in the bis-Tris buffer solution is obtained from Fig. 1(b) in Ref. [15].

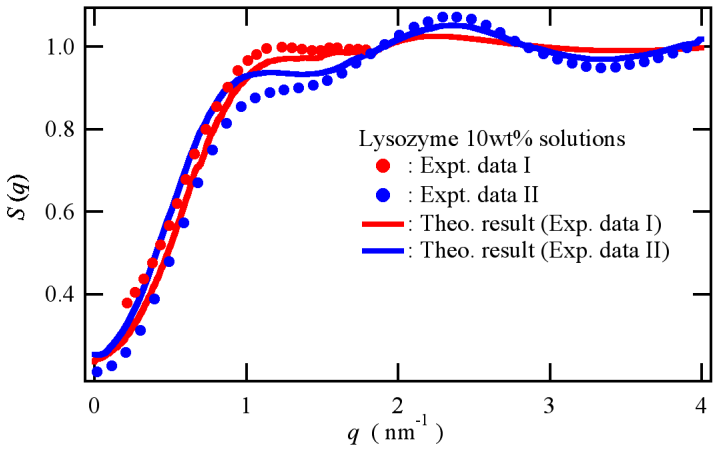

Figure 2. (a) Radial distribution functions of proteins $g(r)$ and (b) effective interaction potentials between protein molecules $V(r)/k_BT$ corresponding to the calculated $S(q)$ shown in Fig. 1.

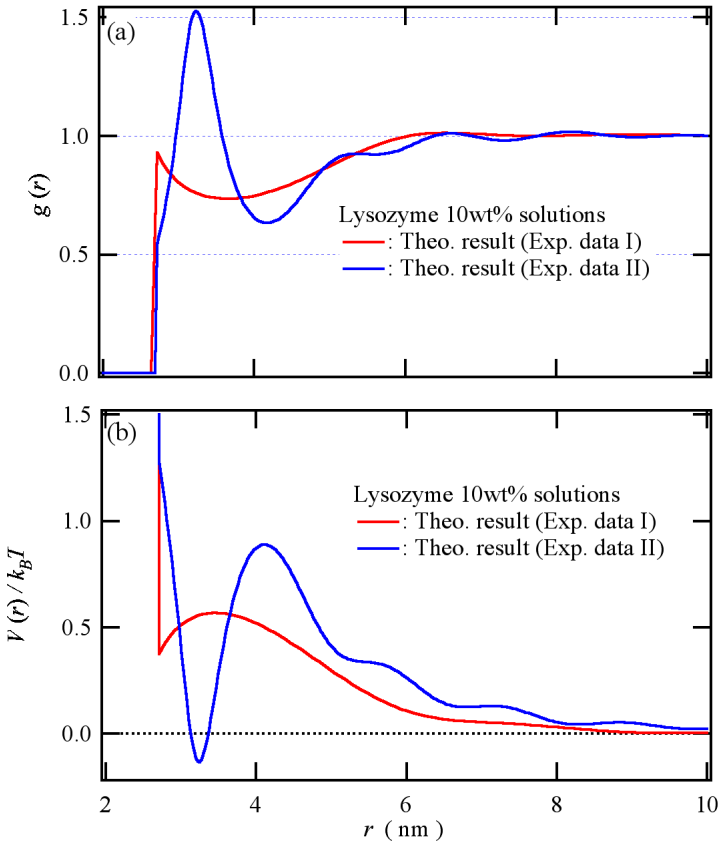

Figure 3. Pressure dependence of experimental $S_{exp}(q)$ for lysozyme 10 wt% solutions at 25 ˚C in bis-Tris buffer. These data are obtained from Fig. 1(b) in Ref. [15]. The inset shows calculated $S(q)$ corresponding to these experimental $S_{exp}(q)$. The red lines, 1 bar; blue lines, 1.5 kbar; and black lines, 3.5 kbar.

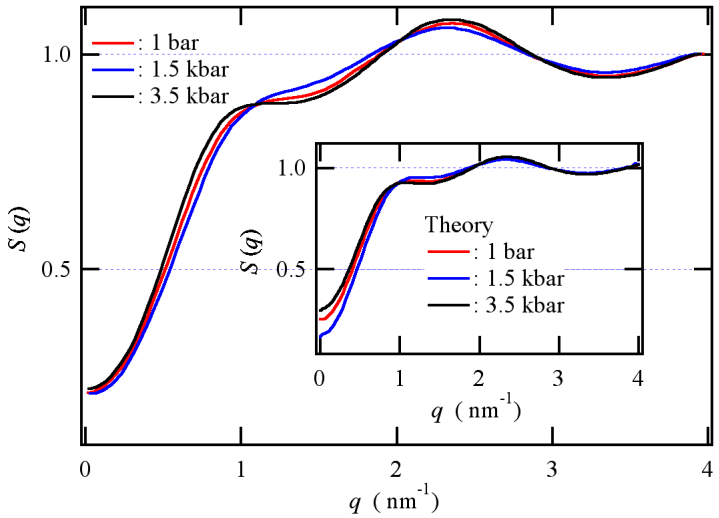

Figure 4. Pressure dependence of (a) the radial distribution functions of proteins $g(r)$ and (b) the effective interaction potentials between protein molecules $V(r)/k_BT$. The red lines, 1 bar; blue lines, 1.5 kbar; light blue, 2.5 kbar; and black lines, 3.5 kbar.

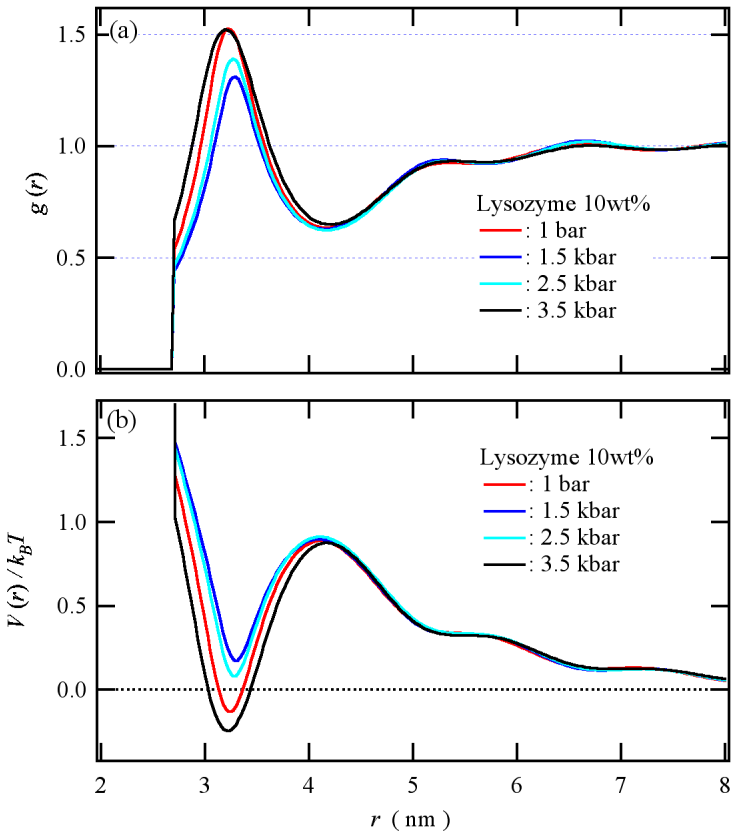

Figure 5. Pressure dependence of (left axis) a value of $V(r)/k_BT$ at the first minimum and (right axis) the distance at the first minimum of $V(r)/k_BT$. The blue and red circles indicate the first minimum values of $V(r)/k_BT$ and the first minimum distance of $V(r)/k_BT$, respectively. The blue and red lines show fitting curves with cubic spline to guide the eye.

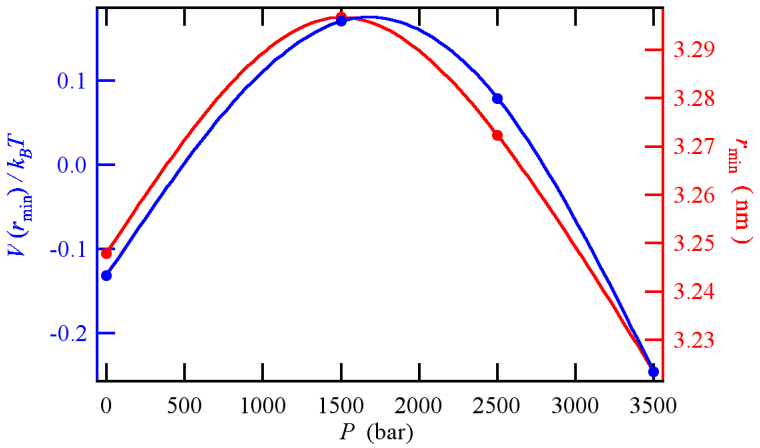

REFERENCES

[1] M. V. Petoukhov and D. I. Svergun, Curr. Opin. Struct. Biol. 17, (2007) 562–571.

[2] D. A. Jacques and J. Trewhella, Protein Science 19, (2010) 642–657.

[3] A. Tardieu, F. Vérétout, B. Krop, and C. Slingsby, Eur. Biophys. J. 21, (1992) 1–12.

[4] O. D. Velev, E. W. Kaler, and A. M. Lenhoff, Biophys. J. 75, (1999) 2682–2697.

[5] F. Bonneté, S. Finet, and A. Tardieu, J. Cryst. Growth 196 (1999) 403–414.

[6] A. Tardieu, S. Finet, and F. Bonneté, J. Cryst. Growth 232 (2001) 1–9.

[7] J. Narayanan, and X. Y. Liu, Biophys. J. 84 (2003) 523–532.

[8] A. Strander, H. Sedgwick, F. Cardinaux, W. C. Poon, S. U. Egelhaaf, and P. Schurtenberger, Nature 432 (2004) 492–495.

[9] F. Bonneté, N. Ferté, J. P. Astier, S. Veesler, J. Phys. IV France 118 (2004) 3–13.

[10] M. Carpineti and Roberto, Phys. Chem. Chem. Phys. 6 (2004) 1506–1511.

[11] M. Niebuhr and M. H. J. Koch, Biophys. J. 89 (2005) 1978–1983.

[12] N. Javid, K. Vogtt, C. Krywka, M. Tolan, and R. Winter, Phys. Rev. Lett. 99 (2007) 028101-1, 028101-4.

[13] A. Shukla, E. Mykonas, E. Di Cola, S. Finet, P. Timmines, T. Narayanan, and D. Svergun, Proc. Natl. Acad. Sci. USA 105 (2008) 5075–5080.

[14] M. G. Ortore, F. Spinozzi, P. Mariani, A. Paciaroni, L. R. S. Barbosa, H. Amenitsch, M. Steinhart, J. Ollivier, and D. Russo, J. R. Soc. Interface 6 (2009) S619–S634.

[15] M. A. Schroer, J. Markgraf, D. C. F. Wieland, C. J. Sahle, J. Möller, M. Paulus, M. Tolan, and R.

Winter, Phys. Rev. Lett. 106 (2011) 178102-1–178102-4.

[16] T. Fukasawa and T. Sato, Phys. Chem. Chem. Phys. 13 (2011) 3187–3196.

[17] J. Möller, M. A. Schroer, M. Erlkamp, S. Grobrlny, M. Paulus, S. Tiemeyer, F. J. Wirkert, M. Tolan, and R. Winter, Biophys. J. 102 (2012) 2641–2648.

[18] V. K. Kelkar, J. Narayanan, and C. Manohar, Langmuir 9 (1992) 2210–2214.

[19] E. J. W. Verwey and J. T. G. Overbeek, Theory of the Stability of Lyophobic Colloids, (Elsevier, Amsterdam, 1948).

[20] H. Imamura, T. Morita, T. Sumi, Y. Isogai, M. Kato, and K. Nishikawa, J. Sync. Rad. 20 (2013) 919–922.

[21] L. Verlet, Mol. Phys. 41, (1980) 183-190.

[22] N. Choudhury and S. K. Ghosh, J. Chem. Phys., 116 (2002) 8517–8522.

[23] J. -P. Hansen and I. R. McDonald, Theory of Simple Liquids, 2nd Ed. (Academic Press, London, 1990).

[24] T. Sumi and H. Sekino, J. Chem. Phys., 126 (2007) 144508-1–144508-7.